

Institute of Polar Studies

Report No. 30

EFFECTS OF A LANDSLIDE ON SHERMAN GLACIER, ALASKA

by

^v
Cedomir Marangunic
Institute of Polar Studies

June, 1972



**GOLDTHWAIT POLAR LIBRARY
BYRD POLAR RESEARCH CENTER
THE OHIO STATE UNIVERSITY
1090 CARMACK ROAD
COLUMBUS, OHIO 43210 USA**

**The Ohio State University
Research Foundation
Columbus, Ohio 43212**

INSTITUTE OF POLAR STUDIES

Report No. 30

EFFECTS OF A LANDSLIDE ON
SHERMAN GLACIER, ALASKA

by

Čedomir Marangunic'

Institute of Polar Studies
The Ohio State University

June 1972

The Ohio State University
Research Foundation

Columbus, Ohio 43212

ABSTRACT

The Alaska earthquake of March 27, 1964, triggered several landslides in the Chugach Mountains of south-central Alaska. One of the largest now covers 8.5 km^2 , about one-third of the ablation zone of Sherman Glacier. Investigations were made in the summers of 1965, 1966, and 1967 of the mechanics of deposition of this landslide material, and the effect of the landslide on the regime of the glacier.

The thickness of the rock debris is a remarkably uniform 1.3 m over most of the area of the slide. Over all of the slide area except the edges, the slide material overlies undisturbed snow that was deposited in the winter of 1963-64. These observations and many of the surface features on the slide indicate that the sliding mechanism was that of an airborne fluidized layer, in which the settling velocity was probably 340 km/hour.

Before the earthquake the mass balance of the glacier was slightly negative; the glacier was receding about 25 m/year and the surface near the snout was lowering by more than 2 m/year. At that time the annual ablation over the area now covered by the slide averaged about 4 m of ice. The debris cover has reduced the annual melting to only a few centimeters and the mass balance for the two years 1964-65 and 1965-66 was positive. The exceptional weather in the 1966-67 balance year produced a strongly negative balance. The stratification of firn and ice suggests that strongly negative balance years occur about once every four years. In the three positive net balance years combined, the glacier gains about $324 \times 10^{11} \text{ g}$, while in the single adverse year it loses about $400 \times 10^{11} \text{ g}$. If this cycle continues, even with the protective debris cover, the net mass balance of the glacier will remain negative.

In the debris-free ablation zone the main sources of heat energy producing ablation are radiation, 48.4 percent, and turbulent heat transfer, 48.1 percent.

The glacier is already responding to the mass gain in the ablation zone associated with the insulating debris cover. Its terminus has advanced 20 m from the summer 1966 position. Across the debris zone surface velocities increase by 25 percent toward the glacier snout. Surface strain nets also indicate that the glacier is extending and new sets of crevasses are being formed in response to the changing stress field. This increase of velocity toward the snout is not a stable situation. The glacier snout will continue to advance, possibly by about 2 km.

Summer surface ice velocities on the glacier are generally larger than annual velocities. Basal sliding amounts to about 80 percent of the surface velocities; therefore, larger summer velocities are probably a reflection of changes in basal sliding produced by a water layer less than 0.5 cm thick.

ACKNOWLEDGMENTS

This research was made possible by National Science Foundation grants GP-4396, GA-409, and GA-983, in 1965-1966, 1966-1967, and 1967-1968, respectively, and was also supported by the Institute of Polar Studies, The Ohio State University.

The author gratefully acknowledges personal financial support from the National Science Foundation in the form of scholarship grants (GA-1275).

The University of Chile awarded the author an extended leave of absence as well as financial support, and travel costs to and from the United States have been financed by the Instituto Antártico Chileno.

Dr. Colin Bull, former Director of the Institute of Polar Studies, supervisor of the Sherman Glacier projects, and adviser of this dissertation, has counseled the author in all stages of the investigation. Dr. Richard P. Goldthwait, a co-supervisor of the original project, has repeatedly offered his critical advice.

Many members of the Institute of Polar Studies and the Geology Department of The Ohio State University have given assistance in various ways. Special mention is made of Dr. Arthur Mirsky, former Assistant Director of the Institute. Mr. John Splettstoesser, present Assistant Director, and Miss Peggy Meehan and Mr. Herbert Mehrling of the Institute staff.

The Ohio State University Numerical Computation Laboratory provided free use of its facilities.

During the summer of 1965 some of the field work was done in cooperation with a party from Muskingum College, New Concord, Ohio, which was carrying out glacial geology and related studies in the area. The party leader, Samuel J. Tuthill, gave much of his time to us and generously offered the support of his helicopter. Dr. William O. Field of the American Geographical Society repeatedly visited and surveyed the terminus of Sherman Glacier. Through the years we have enjoyed his full cooperation and assistance.

The 1965 field party consisted of Messrs. George Markarian and James Westwater (field assistants) and the writer. Dr. Colin Bull, supervisor of the project, spent part of the season with the team. The 1966 party consisted of Messrs. James Westwater and Leslie Morris (assistants) and the writer. The 1967 field party consisted of Messrs. Robert Ellis and Maurice McSaveney (assistants), and the writer; Dr. Colin Bull again spent part of the summer on the glacier. In 1968, Dr. Colin Bull and the writer spent six days on the glacier.

Dr. Colin Bull, Dr. James W. Collinson, Dr. Robert J. Fleck and Dr. Richard P. Goldthwait reviewed the manuscript and gave valuable advice.

CONTENTS

	Page
ABSTRACT	ii
ACKNOWLEDGMENTS	iii
INTRODUCTION	1
Outline of the Field Work	1
Names of Tributary Glaciers	2
GENERAL CHARACTERISTICS OF THE GLACIER	5
Location and Magnitude	5
Classification	5
Past Behavior	5
SURVEY WORK	9
Triangulation Network	9
Triangulation Network Scheme	11
Station Markers	11
Coordinates and Azimuths	11
Base Line Measurements	12
Measurements of Horizontal and Vertical Angles and Station Adjustments	12
Adjustment of Network Figures	12
Strength of Figures	13
Computations of Horizontal Distances and Coordinates	15
Horizontal Adjustment of the Triangulation	16
Computation of Elevations	17
Adjustment of Elevations	17
Surface Velocities	18
Surface Markers Network	18
Measurements	19
Computation of Velocities	19
Additional Survey Work	20
Results	20
GRAVITY SURVEY AND THICKNESS OF THE GLACIER	21
Gravity Stations	21
Base Station	21
Traverse Stations	21

CONTENTS (Continued)

	Page
Measurements of Gravity	26
Reduction of Gravity Data	26
Ice and Rock Densities	26
Free-Air Correction	27
Bouguer Correction	28
Theoretical Gravity and Latitude Correction	28
Terrain Corrections	28
Bouguer Anomalies	29
Interpretation of the Anomalies	30
Results and Accuracy.	33
METEOROLOGICAL AND SHORT-TERM ABLATION OBSERVATIONS	35
Stations and Observation Programs	35
Temperature	37
Humidity	49
Atmospheric Pressure	49
Sunshine	54
Clouds and Cloudiness	54
Precipitation	54
Wind Speed and Direction	61
Short-Wave Radiation	63
Surface Ablation	63
SURFACE HEAT BALANCE	69
Surface Heat Balance at Upper Ice Station	69
Heat Balance Computations	69
Net Short-Wave Radiation	69
Net Long-Wave Radiation	70
Turbulent Transfer of Sensible Heat	70
Turbulent Transfer of Latent Heat	72
Heat Contributed by Precipitation	73
Heat Sink	73
Results	73

CONTENTS (Continued)

	Page
Surface Heat Balance at Lower Ice Station	77
DEBRIS SLIDE	79
Origin and Characteristics	79
Transport Mechanism	84
Definition of Terms	84
Movement of the Landslide	87
Minimum Sliding Velocity and Fluidization	89
Sliding Mechanism	90
Discussion	90
Other Landslides	91
Comparison with other Slides	92
GLACIOLOGY.	95
Mass Balance in the 1966-1967 Budget Year	95
Heat Flow Through the Debris Cover and Sub-Debris	
Ablation	95
Measurements on Debris-Free Areas	97
Mass Balance	98
Surface Ice Velocities	100
Seasonal Variations of Surface Velocities	100
Variations of Surface Velocities Along the Glacier	103
Direction of Motion of Surface Markers	105
Englacial Velocities and the Flow Law of Glacier Ice	105
Surface Strain Rates	106
Layout of Strain Nets	108
Computation of Strain Rates and Stresses from Strain	
Nets	108
Strain Rates by Velocity Gradient Method	112
Bottom Shear Stresses	113
Changes at the Terminus	113
Major Structures of the Glacier	115
Dirty Ice Layers and Dirt Bands	115
Foliation	118
Crevasses	120
Ogives	123

CONTENTS (Continued)

	Page
FUTURE BEHAVIOR OF THE GLACIER	125
Changes at the Terminus	125
Eastern Edge of the Debris	126
Debris-Covered Ice as an Isolated Glacier	126
Future Behavior: An Integrated View	127
CONCLUSIONS	129
Summary	129
Suggestions for Future Work	130
REFERENCES	131

ILLUSTRATIONS

Figure		Page
1	Map of Sherman Glacier	3
2	Aerial Photograph of Sherman Glacier	6
3	Triangulation Network, Sherman Glacier	10
4	Computation of Coordinates of Survey Stations	15
5	Adjustment of Elevations in Quadrangles	18
6	Gravity Base Station on Sherman Glacier	22
7	Longitudinal and Transverse Profiles of Sherman Glacier from Gravimeter Survey	31
8	Longitudinal and Transverse Profiles of Andres Glacier from Gravimeter Survey	32
9	Daily Air Temperature, 1965	39
10	Daily Air Temperature, 1966	40
11	Daily Air Temperature, 1967	41
12	Five-day Averages of Air Temperature, 1966	43
13	Five-day Averages of Air Temperature, 1967	44
14	Comparison of Five-day Averages of Air Temperature, 1965.	45
15	Comparison of Five-day Averages of Air Temperature, 1966.	46
16	Comparison of Five-day Averages of Air Temperature, 1967.	47
17	Diurnal Variation of Mean Air Temperature	48
18	Mean Daily Relative Humidity	51
19	Rain, Sunshine and Sky Cover, 1965	56
20	Rain, Sunshine and Sky Cover, 1966	57
21	Rain, Sunshine and Sky Cover, 1967	58
22	Frequency Percent of Cloudiness at the Meteorological Station on Debris Slide, Sherman Glacier, Summers 1965, 1966, 1967.	59

ILLUSTRATIONS (Continued)

Figure		Page
23	Wind Roses	62
24	Ablatograph at Upper Ice Station	65
25	Ablation Summary	66
26	Geologic Structure of Shattered Peak Ridge	80
27	Vertical Photo of Debris Slide on Sherman Glacier, Alaska. Arrow Indicates Origin of Main Slide and Direc- tion of Movement. Aerial Photography by Austin S. Post, U.S. Geological Survey, September 1966.	82
28	Cone on Debris Slide.	83
29	Winter 1963-1964 Snow Under Debris Slide.	85
30	Profile of the Eastern Debris Edge Near Marker 51	86
31	Stratigraphy and Temperature Profile in Pit West of Pole 16	96
32	Ablation-Accumulation Map, Sherman Glacier	99
33	Motion of Surface Markers	101
34	Surface Velocities and Elevations Along the Centerline of Sherman Glacier	102
35	Positions of the Terminus	114
36	Dirt Bands and Ogives in the Upper Part of Sherman Glacier	116
37	Attitude of Foliation Near Base Camp	119
38	Crevasse Pattern.	122

TABLES

Table	Page
1 Strength of Figure Values and Best Paths Through Triangulation Net	14
2 Gravity Stations and Ice Thicknesses Along the Lower Longitudinal Traverse, Sherman Glacier, August 25, 1966 . .	23
3 Gravity Stations and Ice Thicknesses Along Various Traverses, Sherman and Andres Glaciers, August and September 1966 . .	24
4 Rock Densities	27
5 Air Temperature Statistics ($^{\circ}\text{C}$)	38
6 Relative Humidity Statistics (%)	50
7 Atmospheric Pressure, Summer 1966	52
8 Atmospheric Pressure, Summer 1967	53
9 Estimate of Sunshine Duration, Base Camp Station	55
10 Frequencies of Dominant Cloud Types, Base Camp Station, from 0600 and 1800 Hours	55
11 Precipitation at Base Camp Station	60
12 Incoming Short-Wave Radiation, Base Camp Station, 1967; 12-Hour Averages for 0600-1800 and 1800-0600 Hours ($\text{Cal}/\text{Cm}^{-2}/\text{Min}^{-1}$)	64
13 Heat Balance, Upper Ice Station	74
14 Heat Balance, Lower Ice Station	77
15 Mass Balance	100
16 Basal Sliding and Bottom Shear Stress	107
17 Strain Rates and Stresses from Strain Nets	109

INTRODUCTION

The Alaska earthquake of March 27, 1964, released a landslide that covered a large part of the ablation area of Sherman Glacier in south-central Alaska. It was immediately recognized that the landslide would produce a change in the regime of the ablation zone of the glacier, and an investigation was started in 1965 to examine the actual conditions on the glacier, the response of the glacier as a whole to this change in the regime of one part, and to predict its future behavior.

The landslide itself presented interesting features which required explanation, and much work has been devoted to understanding its sliding mechanism.

Field work was carried out each summer since 1965, and it is hoped that the observations will be continued to determine more completely the behavior of the glacier as it advances in response to the changed regime.

The epicenter of the earthquake was in Prince William Sound, about 130 km northwest of Cordova, where it reached an intensity of VI on the Mercalli scale (Plafker, 1968). The earthquake produced "tectonic uplift" (Plafker, 1965) of 2 to 3 m in the Cordova area.

Outline of the Field Work

The first summer was devoted mainly to establishing a triangulation net on the hills surrounding the glacier and laying out networks of markers on the glacier for determining surface velocity, and for direct measurement of strain. A modest meteorological program was undertaken and preliminary investigations were made.

In 1966 the debris slide was studied in more detail. The meteorological program was enlarged to assess the changes introduced by the debris cover to the climatic pattern of the area. A gravity survey was undertaken to determine the thickness of the glacier, and investigations of mass balance and surface movements were continued.

In 1967 the field work was directed toward some of the remaining problems of the transport mechanism of the debris slide, a study of the heat balance at the glacier surface, and the assessment of accumulation on the tributary glaciers. Much of the time was spent resurveying the triangulation net more accurately than in 1965. Glaciological work of the previous summers was continued.

A short 1968 season was spent in resurveying markers on the debris slide and in the ablation zone of the glacier, and redrilling them for resurvey in 1969.

Much of this report constitutes the dissertation of Marangunic' (1968) of The Ohio State University. For details on surveying such as base lines, observed angles, and computer programs for centering eccentric stations and adjustment of quadrangles, the reader is referred to the Appendixes of the dissertation. This report is concerned mainly with the results of the first three summers work (1965, 1966, 1967).

Names of Tributary Glaciers

In the course of our field work, and in subsequent reports, the need for names for the tributary glaciers was felt. Names honoring the achievements and the people of the early Spanish explorations that led to the discovery of Cordova Bay have been proposed to the U. S. Board on Geographic Names. Five southern tributaries are named from west to east: Fidalgo, Andres, Eliza, Melendez and Carlos. The five northern tributaries are named from west to east: Ana, Serantes, Mondofia, Margarita and Favorita (Fig. 1).

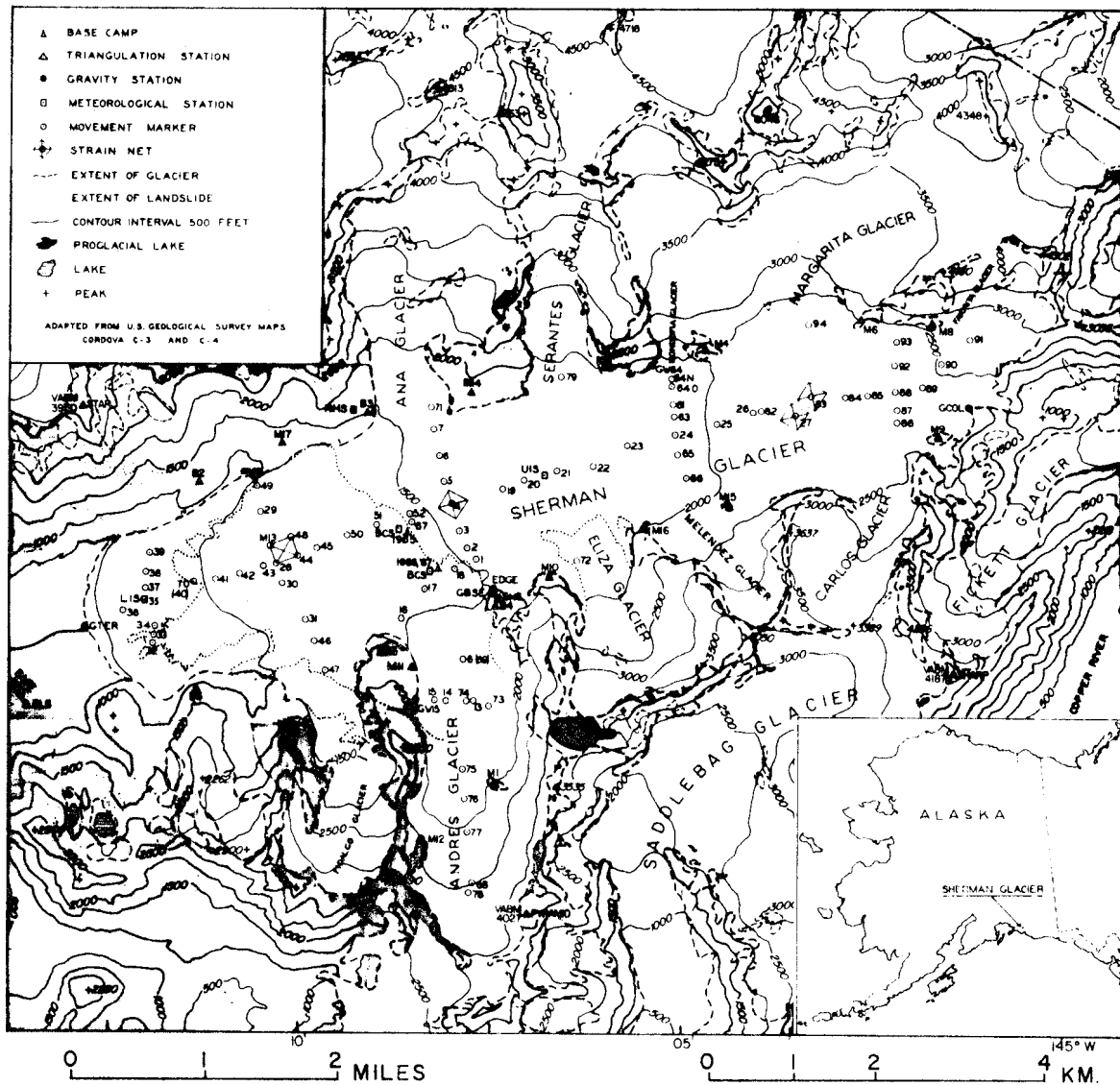


Fig. 1. Map of Sherman Glacier.

GENERAL CHARACTERISTICS OF THE GLACIER

LOCATION AND MAGNITUDE

Sherman Glacier is located in the Chugach Mountains of south-central Alaska, about 35 km northeast of Cordova. It lies approximately at 60°33' N and 145°05' W.

The glacier and its tributaries, except the first southern tributary, cover an area of 54.1 km². Sherman Glacier flows westward, falling in surface elevation from about 725 m at the col leading to the Copper River delta, to about 112 m at its terminus (Fig. 2). The highest peaks in the area reach about 1900 m in the range enclosing the Sherman Glacier basin on the north. There are no large snow accumulation areas above 1400 m.

Sherman Glacier alone is 11 km long and averages 2 km in width. Before the landslide the surface sloped evenly, the slope being about 2° over most of the glacier and increasing to about 6° near the snout. Since 1964 the surface in the ablation zone and the snout have changed progressively due to the effect of the landslide debris cover.

CLASSIFICATION

According to Ahlmann's (1948) classification, the Sherman is a valley or alpine glacier type III. He describes this type of glacier as having ... "no proper firn basin; avalanches from the steep, very high valley sides replace them." On Sherman Glacier avalanches are not significant; the alimentation of Sherman Glacier is produced by tributary glaciers joining the Sherman from the north and south. Geophysically, the Sherman is a temperate glacier. No temperatures have been measured at depth, but the glacier is at low latitude and elevation, and meltwater is abundant during summer; therefore, the glacier may be assumed to be at its pressure-melting point throughout.

PAST BEHAVIOR

The recent behavior of the Sherman Glacier has been studied by Tuthill and others (1968). Following is a summary of their conclusions.

The glacier reached a maximum around the year 1700, in a position about 1.5 km from the 1965 terminus. By 1941 the terminus had receded 725 m from the 1700 position. By 1950 the terminus had retreated an additional 275 m and lay 375 m ahead of its 1965 position. There seems to have been a steady withdrawal from 1700 to 1964, interrupted only by a slight advance in 1930 to a position somewhat ahead of the 1941 terminus.



Fig. 2. Aerial photograph of Sherman Glacier
(by A.S. Post, U.S. Geol. Survey, 1966).

The recession rates are:

1890 to 1941	13 m yr ⁻¹
1941 to 1950	31 m yr ⁻¹
1950 to 1965	25 m yr ⁻¹

From 1900 to 1950 surface lowering averaged 2.5 m near the 1950 terminus, 2.1 m 300 m from the terminus, and about 1 m in the interval 900 m to 2500 m from the terminus.

From 1950 to 1965 surface lowering averaged from 4.1 m near the 1965 terminus to about 1.7 m near the 1965 position of the western edge of the debris slide.

SURVEY WORK

A triangulation network was established along the edges of the glacier. From the stations of this triangulation net the location of points on the glacier were measured repeatedly to determine the horizontal components of their velocity.

TRIANGULATION NETWORK

In the summer of 1965 a party from Muskingum College, New Concord, Ohio, led by S. J. Tuthill, studied the glacial geology of the area between the Sherman and Sheridan glaciers. They measured a base line 713.93 m long on the outwash plain between the glaciers, and, cooperating with the Institute of Polar Studies party, established five survey stations around the lower part of the ablation area of Sherman Glacier (B2, B3, B4, B5 and B6). The Institute of Polar Studies party established 13 more survey stations (M1, M4, M5, M6, M8, M9, M10, M11, M12, M14, M15, M16, and M17) on hillsides around the margins of Sherman Glacier and its tributary, Andres Glacier (see Fig. 3). Another survey station marker, M13, set up near the center of the slide, has been used as a corner of a strain net.

The Institute's party used a DKM-1 theodolite and the Muskingum College party used a Wild T-2 theodolite.

Dr. W. O. Field of the American Geographical Society, accompanying the Muskingum College party in 1965, established nine survey and photo stations around the terminus of the glacier in order to record changes in its position. In 1966 and 1967 the Institute of Polar Studies party reoccupied some of Dr. Field's stations. The stations were occupied again in 1968 by Dr. Field but his data are not included here.

In 1965 a panorama of photographs, covering at least 180°, was taken with a 135 mm focal length camera mounted on the theodolite tripod from most of the survey stations surrounding the glacier. The panoramas were repeated in 1966 at a few of the stations.

In 1967 aerial photographs of mapping quality covering the whole of Sherman Glacier and its tributaries were taken by Air Photo Tech, Inc., of Anchorage, Alaska. Both line and ortho photo topographic maps of the glacier at 1:10,000 scale with a 5-m contour interval were produced by Mr. Henry H. Brecher from these photographs. For this purpose, the quality of the triangulation was improved in 1967 by resurveying the entire network with a Wild T-2 theodolite, and measuring an additional base line for control of scale, at the eastern end of the network between stations M8 and M9 (see Fig. 3). On the outwash plain one end of the existing base line was inaccessible without a helicopter, so a new base line (387.082 m long) was set up between stations BLS and BLN (Fig. 3).

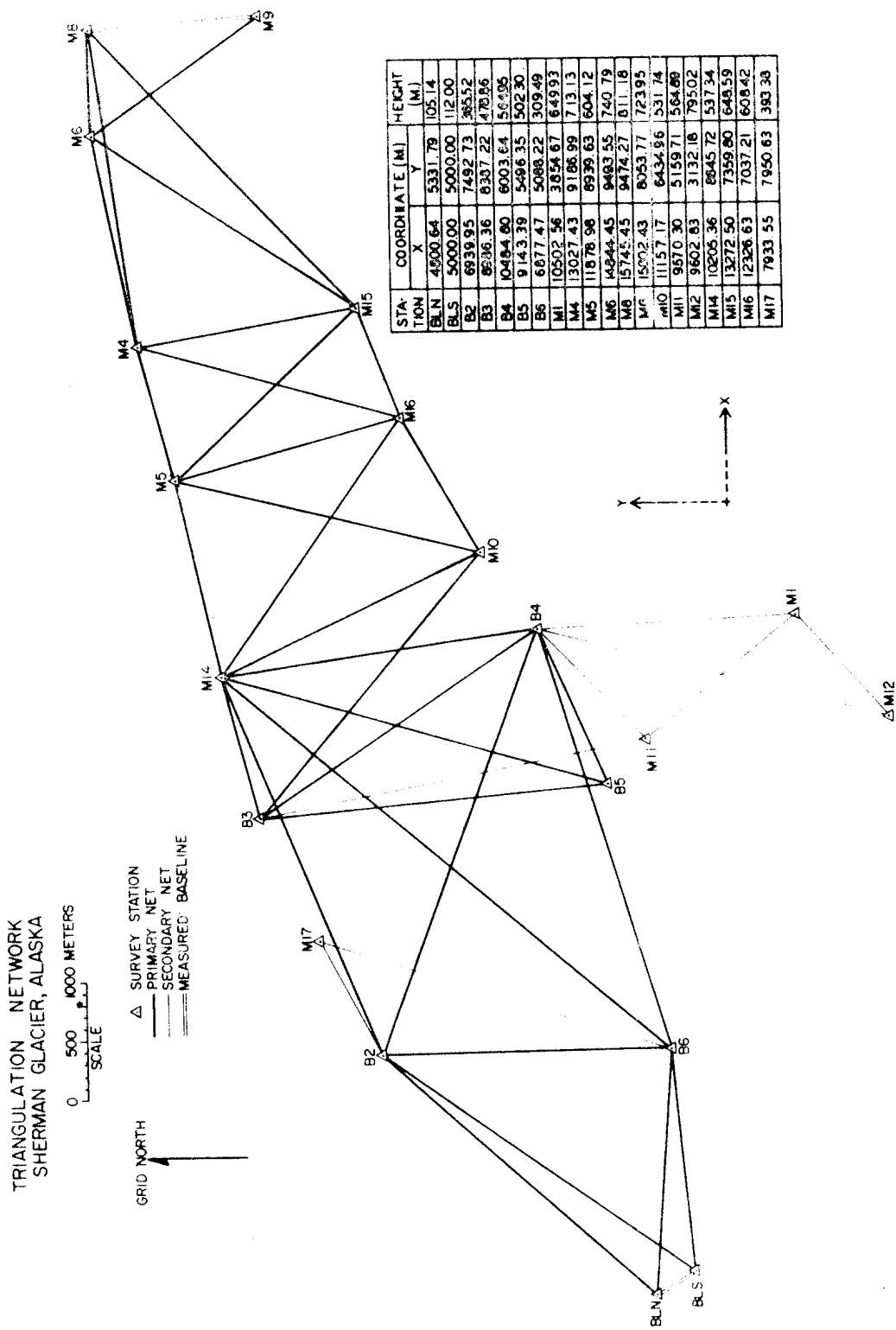


Fig. 3. Triangulation Network, Sherman Glacier.

Before the aerial photography in 1967, stations BLS, BLN, M9, M14, and M15 were marked with crosses of white cloth with arms 12 m long and 2 m wide. The stations are thus plainly visible in the aerial photographs.

Triangulation Network Scheme

The primary triangulation net consists of six braced quadrilaterals and two triangles, extending from the base line on the outwash of Sherman Glacier up the glacier to the col leading to the Copper River delta, where the second base line was measured.

The lengths of the lines within the figures, except for the short base line in the outwash, range from about 1000 m to nearly 4000 m. The length of the whole network, from station BLS to station M8, is nearly 12,000 m; the error in this length introduced by ignoring the spherical figure of the earth is less than 5 cm, less than the likely error of the observations. The survey computations have therefore been carried out as for plane figures.

Station Markers

Stations erected by the Muskingum College party (B2 to B6), consist of two 1-foot (0.3-m) square pieces of plywood on a 6-foot (1.8-m) long, 2 in. x 2 in. (5 cm x 5 cm) stake, inserted in a yellow painted rock cairn. These stations were considered eccentric; angles read at these stations were centered by a SCATTRAN-language computer program which corrected the directions (cf. Breed and others, 1962).

The M stations, erected by the Institute of Polar Studies party, consist of a 6-foot (1.8-m) long, 4 in. x 4 in. (10.2 cm x 10.2 cm) red stake, on a wooden base with a strong nail which fits into a hole in the base of the stake. The stakes are wired down to steel pegs and are easily detached from the base, so that the base may be occupied as a conventional station, with the nail as reference marker. Station M15, which lacks a base, is occupied as either a conventional or as an eccentric station.

Coordinates and Azimuths

Since no position or azimuth observations were made, a local coordinate system was established by projecting the network, first calculated with a random azimuth, on a U.S. Geological Survey topographic map 1:63,360, Cordova C-3 and C-4. The azimuth of the line from BLS to BLN was thus set as $329^{\circ}00'00''$. It is estimated that the azimuth has a maximum error of $\pm 2^{\circ}$.

Base Line Measurements

Base lines were measured by triangulation methods, with a Wild 2-m subtense bar and a Wild T-2 theodolite.

The base line on the outwash plain, between stations BLS and BLN, was determined by measuring the distance (87.694 m) between an offset station and the subtense bar located on BLN, and then expanding this distance by triangulating the figure BLS-BLN-offset station. All angles, including the one subtended at the offset station by the two ends of the subtense bar, were obtained from four sets of measurements, each consisting of the mean of a set of direct and reverse observations. The expanded base line between BLN and BLS is 387.082 m long. The expansion ratio is 3.3.

The base line in the col to the Copper River was measured in a similar way. The triangulation figure was nearly a right-angle triangle, with the hypotenuse being between M8 and the offset station west of M9. The subtense bar was located at the offset station, and the distance between it and M9 was 123.917 m. The expanded base line between M8 and M9 is 1421.641 m long. The expansion ratio is 11.5. The angles were obtained from three sets of angles measured from M9 (nine sets for the subtended angle), six sets measured from the offset station, and five sets from M8.

Measurements of Horizontal and Vertical

Angles and Station Adjustments

The individual figures of the triangulation network were surveyed by observing all horizontal and vertical angles within them. At least two sets of horizontal observations were made from each station, a set consisting of advancing the theodolite in direct position from left to right until reaching the starting point, and then reversing the theodolite and swinging from right to left. The maximum accepted error in the closing of the circles was 5 seconds.

The mean horizontal angles from all sets of measurements at a station were averaged, and these averaged angles added up. The departure from 360° was usually less than 10 seconds and was distributed equally among the angles of the circle.

Mean vertical angles obtained from two sets of observations, each one comprising direct and reverse readings, were averaged. The difference between the sets of vertical angles was usually less than 5 seconds.

Adjustment of Network Figures

Triangles were adjusted by dividing the error of closure equally among the three angles, so that the corrected angles totalled 180°.

The quadrilaterals were adjusted separately by the angle-and-side-adjusting method of Wright and Hayford (in: Breed and others, 1962); a SCATRAN-language computer program was written for this purpose. The computer output gives the adjusted angles to one hundredth of a second. For computation of the triangulation net, angles were rounded to full seconds, checking that totals from each station still were 360°.

Strength of Figures

The configuration of the triangles and the relationships of the triangles within the quadrangles determine the accuracy with which the computation of a triangulation is carried out. The U. S. Coast and Geodetic Survey (Reynolds, 1928) method of finding the best route by which the computation should be carried through the quadrangles has been used.

The method consists of testing the strength of different chains of triangles by computing the probable error of a triangle side. The measure of strength of figure, R , is given by:

$$R = \frac{D - C}{D} \times \Sigma (\delta A^2 + \delta A \delta B + \delta B^2),$$

where D is the total number of observed directions from each station in the figure less two (the observed directions at the two ends of the figure's base line), C is the number of geometric conditions in the figure (see below), and δA and δB are the tabulated differences for one second in the $\log \sin A$ and $\log \sin B$, in the 6th decimal place. A and B are the angles opposite the side to be computed, and the known side, respectively.

The number of geometric conditions, C , is given by:

$$C = (n' - S' + 1) + (n - 2S + 3),$$

where n' is the total number of lines observed in both directions, including the figure's base line, S' is the total number of stations occupied in the figure, n is the total number of lines in the figure including the figure's base line, and S is the total number of stations.

The strongest route for computations, and that used, is that given by the smallest value of R in the figure, R_1 . Table 1 lists the values of R_1 (the best path) and R_2 (the second best route) for the different figures; R_1 was used to compute the sides and coordinates of the stations in the triangulation net.

Excluding the first quadrangle, which has a large R_1 (84.0) due to its short base line, the sum of the R_1 values for the primary network is 69.3. Considering the difficulties of the terrain, this value of R_1 is very satisfactory, being much better than that required for a third-order triangulation which has a maximum limit of 175.

TABLE 1. STRENGTH OF FIGURE VALUES AND BEST PATHS
THROUGH TRIANGULATION NET

Figure	R1	R2	Path of R1		
			From known side	Compute side	Compute side
<u>Primary Network</u>					
Quadrangle: BLS-BLN-B2-B6	84.0	91.8	BLS-BLN	BLN-B6	B6-B2
Quadrangle: B6-B2-M14-B4	9.6	12.6	B2-B6	B2-B4	B4-M19
Quadrangle: M14-B4-B3-B5	1.2	1.8	M14-B4	B4-B3	B3-B5
Triangle: Location of M10	15.8	24.0	B3-M14	B3-M10	
Quadrangle: M14-M10-M5-M16	3.0	3.6	M10-M14	M14-M16	M16-M5
Quadrangle: M5-M16-M15-M14	3.0	3.0	M5-M16	M5-M15	M15-M4
Quadrangle: M15-M4-M6-M8	42.0	61.8	M4-M15	M15-M8	M8-M6
Triangle: Location of M9	14.7	14.7	M6-M8	M8-M9	
<u>Secondary Network</u>					
Triangle: Location of M17	2.3	45.0	B2-B6	B6-M17	
Triangle: Location of M11	0.8	30.0	B3-B4	B3-M11	
Triangle: Location of M1	6.8	13.5	B4-M11	M11-M1	
Triangle: Location of M12	5.3	53.3	B4-M1	B4-M12	

Computations of Horizontal Distances

and Coordinates

As mentioned previously, station BLS was chosen as the point of origin for the whole network, and its coordinates were set as X (grid east direction) 5,000.000 m and Y (grid north direction) 5,000.000 m. The azimuth from BLS to BLN was taken to be 329° . The length of the measured base line, BLS to BLN, was 387.082 m. The coordinates of BLN are then:

$$Y_{BLN} = 5,000.000 + 387.082 \times \cos 329^\circ$$

$$X_{BLN} = 5,000.000 + 387.082 \times \sin 329^\circ.$$

The coordinates of the rest of the stations in the triangulation net were computed along the path for the best strength of figure.

From two stations, A and B, of known coordinates, the coordinate of station C can be computed in the following manner:

1. the distance D between stations A and B, of known coordinates X_A , Y_A , X_B , Y_B is:

$$D = \sqrt{(X_A - X_B)^2 + (Y_A - Y_B)^2}$$

2. the azimuth of the new line to station C is obtained by adding the observed forward angle at the reference station to the azimuth of the known line, between stations B and A (Fig. 4):

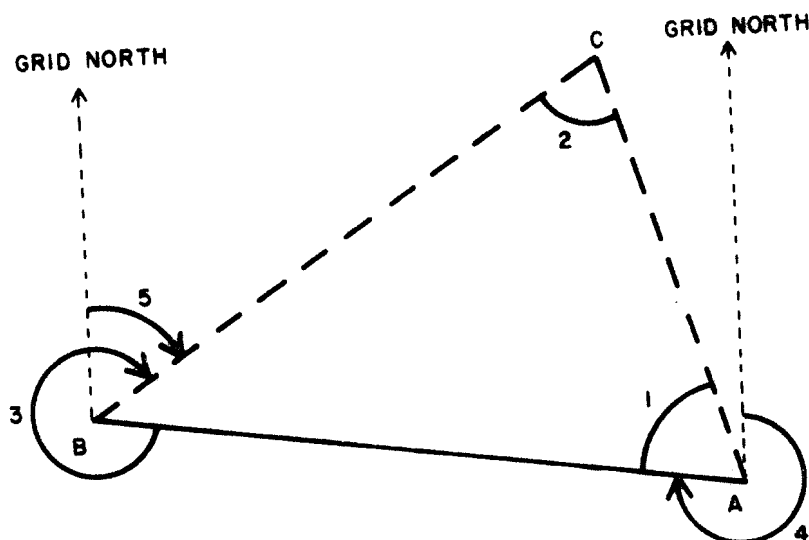


Fig. 4. Computation of Coordinates of Survey Stations.

∠ 4 is the azimuth of the known line between fixed points B and A

∠ 3 is the measured angle from BA to BC

∠ 5 is the azimuth of the new direction BC,

$$\angle 5 = \angle 4 + 180^\circ + \angle 3.$$

3. the distance BC is computed by the sine law

$$BC = \frac{BA \times \sin \angle 1}{\sin \angle 2}$$

with ∠ 1 and ∠ 2 already known.

4. the coordinates of station C are then:

$$X_C = X_B + BC \times \sin \angle 5$$

$$Y_C = Y_B + BC \times \cos \angle 5.$$

Once the coordinates of all stations have been circulated, distance between any two of them can be computed by similar simple trigonometry.

Horizontal Adjustment of the Triangulation

The triangulation network, computed from the BLS-BLN base line toward the east, has been adjusted so that the calculated length of the end line in the net, the distance M8 to M9, equals the measured length of the M8-M9 base line. The difference between measured and calculated distance M8-M9 has been distributed proportionally along the shortest route from BLN to M9, following the path of the best strength of figure.

The total length of the route is the sum of the distances between the stations in the strongest path, namely BLN to B6, B6 to B2, B2 to B4, B4 to M14, M14 to M16, M16 to M5, M5 to M15, M15 to M8, M8 to M9. The correction applied along the path is equal to:

$$COR = \frac{P \times E}{T},$$

where COR is the correction to be applied to a distance between two stations, P is the elapsed length from station BLN, E is the difference between the observed and measured lengths of the distance M8-M9, and T is the total length of the route from BLN to M9.

The azimuths of the lines along the adjusted route are not changed. New coordinates of these stations are computed from the already known azimuths and the adjusted lengths. Coordinates of the stations not located in the path of the adjusted route, and the lengths and azimuths of the lines between all stations, are again computed as already explained.

Computation of Elevations

From the existing U.S. Geological Survey maps (Cordova C-3 and C-4 sheets, 1:63,360), and from altimetry connections with the Mile 13 Cordova Airport, the elevation of BLS has been estimated as 112 m. The error of this estimate is probably ± 1 m.

Elevation differences between the stations have been calculated by averaging the differences computed from reciprocal vertical angles observed from the two ends of a line. Simultaneous reciprocal observations were not made in the triangulation, so that a standard correction for refraction errors has been introduced:

$$F = 0.0675 \times D^2 ,$$

where F is the correction and D the distance between two stations. Sharni (1963) and Brecher (1966) found a 0.065 coefficient value over glaciers, but since ours was a rather mixed terrain, the standard coefficient of 0.0675 has been used.

The elevation difference for a downward (negative) angle is:

$$H_1 = D \times \tan \alpha' - I + T + F .$$

For an upward (positive) angle it is:

$$H_2 = D \times \tan \alpha'' + I - T - F ,$$

where H is the elevation difference, D is the horizontal distance between the stations, I is the instrument height, T is the target height, and α' and α'' are the absolute values of the downward and upward angles respectively, and F is the refraction correction.

The height difference between the two stations is then:

$$\frac{H_1 + H_2}{2} .$$

Adjustment of Elevations

The shortest line in the present survey (BLS to BLN) traverses uniform terrain in the outwash plain. Consequently, the vertical angles between these two stations, free of the additional refraction errors created by air turbulences over ice/snow and rock terrain, are the strongest reciprocal angles in the network. Assuming the elevation of BLS to be 112 m, the elevation of BLN has been computed by the method previously described and has been kept fixed.

With two fixed elevations in a figure, the adjustment of the elevations of the other two stations in each quadrangle was completed in the following manner (Fig. 5):

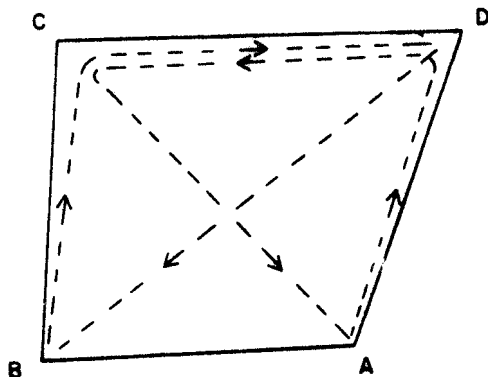


Fig. 5. Adjustment of Elevations in Quadrangles.

B and A are the two stations of fixed elevation. The algebraic sum of the elevation differences along the path B to C, C to D, and D to B should be equal to zero. If not, the error is distributed equally among the elevation differences along the path. The sum along path A-D-C-A is then similarly made equal to zero, and the elevation differences between C and D, computed along the two paths, are averaged. The process of making the sums of both paths equal to zero is then repeated, using the average elevation difference between C and D as a fixed difference. The elevations of C and D are then computed by adding to the elevations of A and B the elevation differences between A and D, and B and C, respectively.

The next quadrangle is then adjusted, using C and D as the fixed elevations.

In triangles, the elevation of the new station is computed from both fixed stations, by adding the elevation differences to the height of each fixed station, and the adjusted elevation of the new station is taken as the average of the two heights thus computed.

SURFACE VELOCITIES

Surface Markers Network

A network of about 80 markers was maintained on the glacier from the summer of 1965 through the summer of 1967, and left for resurvey in the summer of 1968 and later. The markers were flagged aluminum pipes 6 and 12 feet (1.8 and 3.6 m) long and 3/4 inch (1.9 cm) in diameter.

On the debris slide the pipes were inserted in rock cairns. On the ice or snow, holes from about 10 m deep in the snout to about 4 m deep near the equilibrium line, were drilled with a hot-water drill (Kasser, 1960), and strings of pipes were tied together internally by means of nylon cords inserted through each of them.

The network of markers comprises a longitudinal and five transverse lines on Sherman Glacier and a longitudinal and two transverse lines on Andres Glacier. Additional markers were set at the confluences of several tributaries with Sherman Glacier.

Although some of the poles in the accumulation areas were lost and had to be replaced, and some were temporarily lost for the summer of 1966, most of the original 1965 markers were resurveyed during the three summers. Some of the markers were surveyed twice during the summers, for comparison of summer and annual velocities.

Measurements

The determination of position of the velocity markers was made by the intersection method of triangulation, from at least two fixed survey stations. The measurement of the horizontal and vertical angles was done in the same way as for the survey stations, but a larger error, up to 30 seconds, was accepted in the closure of the circles. It was often reached because triangulation commonly was carried out in adverse weather.

The occupation of the two or more stations for fixing the position of a marker was not simultaneous, but, as far as possible, the two stations were occupied within two to six hours. In this time, the position of the markers changed about 4 cm (from summer velocities computed over most of the glacier). It was not considered necessary to introduce adjustments since this error is lower than the observational error. Occasionally, time intervals of up to 24 hours were accepted, but if the six hour time limit was exceeded, the usual procedure was to repeat the survey from the first station.

Computation of Velocities

For each survey horizontal coordinates and elevations of the velocity markers were computed within the grid established in the triangulation network. The magnitude and horizontal and vertical components of motion of each marker between the various surveys have been calculated from the repeated determination of position. However, the vertical component must be corrected for ablation or accumulation. Daily and annual velocities were then abstracted from the time intervals and travel distances. For a description of these computations see, for example, Brecher (1966).

ADDITIONAL SURVEY WORK

It was intended originally to tie the triangulation work to two U.S. Coast and Geodetic Survey stations in the area. However, Pyramid Peak station was lost in a landslide released from that peak during the earthquake, and no marker was visible on the second station, Star Peak, north of the snout of Sherman Glacier. Instead, two high peaks of 6046 feet (1843 m) and 6263 feet (1909 m) north of the glacier, and a smaller, but prominent peak of 2906 feet (886 m) south of the snout of the glacier, were included in the 1966 triangulation work. (Both English and metric units are given for peak elevations -- published maps give elevations in feet.)

Other significant points, such as gravimetry and meteorological stations, were also included in the surveys of the various summers.

A SCATRAN-language computer program was developed to calculate and adjust the triangulation network, and to obtain the velocities of the glacier markers.

RESULTS

The coordinates and elevations of all the triangulation stations are given in Figure 3. The ± 1 m error in the elevation of the whole network arising from the estimate of 112 m for station BLS, is considered acceptable because it is less than the errors introduced by the estimate of the refraction coefficient.

Errors in the horizontal distance computations are indicated by the magnitude of the calculated unadjusted dimension of the line M8 to M9, 1422.826 m, compared with the measured length of 1421.641 m. The error, built up through six quadrangles and two triangles of primary triangulation network, is then 1.185 m.

Horizontal coordinates of the triangulation stations have a ± 20 cm error in the local grid system after adjustment. The U.S. Coast and Geodetic Survey (1964) estimated 6 feet (1.8 m) of upward movement of land relative to sea level in the Cordova area during the Good Friday earthquake. Movement in the Sherman Glacier area is not known and no corrections have been applied to the elevations given in Figure 3.

However, errors in absolute height and position are irrelevant to studies of motion and ablation, and even to local mapping from special photography, as everything can be referred to a local datum.